IOPscience iopscience.iop.org

Home Search Collections Journals About Contact us My IOPscience

Charge-memory effect in a polaron model: equation-of-motion method for Green functions

This content has been downloaded from IOPscience. Please scroll down to see the full text.

2008 New J. Phys. 10 085002

(http://iopscience.iop.org/1367-2630/10/8/085002)

View the table of contents for this issue, or go to the journal homepage for more

Download details:

IP Address: 132.199.103.61
This content was downloaded on 03/05/2017 at 18:52

Please note that terms and conditions apply.

You may also be interested in:

Phonon-assisted spin-polarized tunneling through an interacting quantum dot
W Rudziski

Molecular transport junctions: vibrational effects
Michael Galperin, Mark A Ratner and Abraham Nitzan

Quantum inelastic electron–vibration scattering in molecular wires: Landauer-like versusGreen's function approaches and temperature effects
H Ness

Spectrum and Franck–Condon factors of interacting suspended single-wall carbon nanotubes
Andrea Donarini, Abdullah Yar and Milena Grifoni

Phonon-affected steady-state transport through molecular quantum dots
T Koch, H Fehske and J Loos

The role of many-particle excitations in Coulomb blockaded transport
B Muralidharan, L Siddiqui and A W Ghosh

Magnetoresistance of nanoscale molecular devices based on Aharonov–Bohm interferometry
Oded Hod, Roi Baer and Eran Rabani

Unified description of charge transfer mechanisms and vibronic dynamics in nanoscalejunctions
R Avriller

Asymmetric Coulomb blockade and Kondo temperature of single-molecule transistors
Florian Elste and Felix von Oppen

New Journal of Physics
The open-access journal for physics

Charge-memory effect in a polaron model: equation-of-motion method for Green functions

Pino D'Amico[1,3], **Dmitry A Ryndyk**[1], **Gianaurelio Cuniberti**[2] **and Klaus Richter**[1]

[1] Institute for Theoretical Physics, University of Regensburg, D-93040 Regensburg, Germany
[2] Institute for Material Science and Max Bergmann Center of Biomaterials, Dresden University of Technology, D-01062 Dresden, Germany
E-mail: pino.damico@physik.uni-regensburg.de

New Journal of Physics **10** (2008) 085002 (12pp)
Received 3 April 2008
Published 5 August 2008
Online at http://www.njp.org/
doi:10.1088/1367-2630/10/8/085002

Abstract. We analyze a single-level quantum system placed between metallic leads and strongly coupled to a localized vibrational mode, which models a single-molecule junction or an STM setup. We consider a polaron model describing the interaction between electronic and vibronic degrees of freedom and develop and examine different truncation schemes in the equation-of-motion method within the framework of nonequilibrium Green functions. We show that upon applying gate or bias voltage, it is possible to observe charge-bistability and hysteretic behavior which can be the basis of a charge-memory element. We further perform a systematic analysis of the bistability behavior of the system for different internal parameters such as the electron–vibron and the lead–molecule coupling strength.

[3] Author to whom any correspondence should be addressed.

© IOP Publishing Ltd and Deutsche Physikalische Gesellschaft

Contents

1. Introduction

Within the field of single-molecule electronics [1]–[4], beside experimental progress with regard to vibrational properties and their signatures in transport [5]–[9], related phenomena such as switching, memory effects and hysteretic behavior in molecular junctions have gained increasing importance and attention. Random and controlled switching of single molecules [10]–[12], as well as conformational memory effects [13]–[15] have been recently explored. Related to these effects, there is the so-called charge-memory effect, that is basically a hysteretic behavior of the charge–voltage, respectively, current–voltage characteristics arising from the interplay between the polaron shift and Franck–Condon blockade [16] in the presence of electron–vibron interaction. Several works have recently addressed this interesting feature of molecular junctions, both experimentally [17, 18] and theoretically [19]–[23].

The charge-memory effect can be explained within the framework of a simple single-level polaron model [20], [23]–[25], where the electronic state is coupled to a vibronic mode with frequency ω_0, see the sketch in figure 1. If the energy of the *unoccupied* electron level *without* electron–vibron interaction is ϵ_0, the *occupied* (charged) state of the *interacting system* will have the energy $\epsilon_1 = \epsilon_0 - \epsilon_p$, where ϵ_p is the so-called polaron shift (called also recombination energy). Neutral and charged (polaron) states correspond to local minima of the potential energy surface and get metastable, if the electron–vibron interaction is strong enough. Upon applying an external voltage, one can change the state of this bistable system, an effect that is accompanied by hysteretic charge–voltage and current–voltage curves. In this model, it is not necessary to include Coulomb interaction explicitly, though one can straightforwardly incorporate charging effects.

It was alternatively suggested in [21, 22] that quantum switching between bistable states rather results in telegraph noise at finite voltage than in a memory effect. In a recent paper [23], considering the problem in the weak molecule-to-lead coupling limit, i.e. for the level width $\Gamma \ll \omega_0, \epsilon_p$, we considered the crossover between these two pictures, if one takes into account the timescale of the switching process. Indeed, the switching time τ between the two states of interest should be compared with the characteristic time of the external voltage sweeping, $\tau_s \sim V(t)/(\mathrm{d}V(t)/\mathrm{d}t)$. For $\tau \gg \tau_s$, quantum switching can be neglected, and hysteresis can be

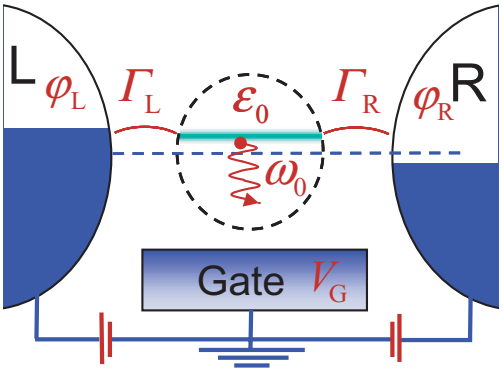

Figure 1. Schematic representation of a single-level model system interacting with a vibronic mode and coupled to left and right leads.

observed, whereas in the opposite limit, $\tau \ll \tau_s$, the averaging removes the hysteresis. In [23], we found that at large enough electron–vibron interaction strength λ/ω_0 (where λ is introduced below in equation (1)), the switching time τ is exponentially large compared to the inverse bare tunneling rate $1/\Gamma$.

In this paper, we consider the polaron problem in another limiting case, $\omega_0 \ll \Gamma < \epsilon_p$, corresponding to the regime where the Born–Oppenheimer approximation holds true. In this situation of intermediate molecule-to-lead coupling, we address the case of time-independent applied voltages, considering then the stationary problem and focusing on the properties of the two states of interest. In this paper, we consider the parameter ranges for which the fluctuations between the two charge states of interest are negligible. It should be noted that the mean-field solutions we consider are metastable, but they are physical in the case of very long switching time τ. Of course, the exact equilibrium solution is a superposition of these two states. We assume that all possible relaxation processes, with the exception of the switching between metastable states, are much faster than τ. Within the framework of nonequilibrium Green functions [26]–[30], we use an equation-of-motion (EOM) approach which allows for studying the appearance of the charge-memory effect addressed at different levels of approximation, starting with the self-consistent Hartree level. The work is partly built on and further develops ideas introduced in [20, 24, 25] and complements the results based on a master equation approach in [23].

The paper is organized as follows: in section 2, we introduce the model and the relevant quantities necessary to describe transport through the molecular junction. In section 3, we outline the EOM method, used for the calculation of nonequilibrium Green functions, and discuss different truncation schemes. In the final section 4, we present and discuss the results of our approach.

2. Model and method

2.1. The single-level electron–vibron Hamiltonian

We consider a three-terminal device with the central part given by a single level interacting with a vibronic mode (see figure 1). Possible experimental implementations include

metal–molecule–metal junctions or scanning tunneling microscopy (STM) spectroscopy of a single molecule on a conducting substrate. To describe such a system we use the standard electron–vibron Hamiltonian

$$\hat{H} = (\epsilon_0 + e\varphi_0)d^\dagger d + \omega_0 a^\dagger a + \lambda(a^\dagger + a)d^\dagger d + \sum_{i,k}\left[(\epsilon_{i,k} + e\varphi_i)c_{i,k}^\dagger c_{i,k} + (V_{i,k}c_{i,k}^\dagger d + \text{h.c.})\right]. \quad (1)$$

Here the first three terms describe the central system including one electronic state with energy ϵ_0, one vibronic state with frequency ω_0 and their mutual interaction with a coupling strength λ. The last term in equation (1) contains the Hamiltonian of the two leads with independent-particle states and the tunneling between the leads and the central region via the couplings $V_{i,k}$. The index i denotes the left and right leads, while k labels the electronic states of electrons in the leads. Below it proves far more convenient to employ the vibronic 'position' and 'momentum' operators

$$x = a^\dagger + a; \quad p = a^\dagger - a. \quad (2)$$

The energy level ϵ_0 in equation (1) can be shifted through the gate voltage V_G. We choose as reference energy $\epsilon_0 = 0$ for $V_G = 0$ and assume a linear capacitive coupling, $\epsilon_0 = \alpha e V_G$ putting $\alpha = 1$. Note that the presence of a bias voltage $V_B = \varphi_L - \varphi_R$ can also change the energy of the electronic level via the parameter $\varphi_0 = \varphi_R + \eta V_B$, where $0 < \eta < 1$ describes the symmetry of the voltage drop across the junction: $\eta = 0$ corresponds to the completely asymmetric case, whereas $\eta = 0.5$ stands for the symmetric case. Thus in all approximations the bias and gate voltages are taken into account twofold, through the potentials of the leads, which can be chosen, e.g. as $\varphi_L = V_B/2$, $\varphi_R = -V_B/2$, and the effective energy of the level, which is correspondingly $\tilde{\epsilon}_0 = \epsilon_0 + e\varphi_0 = eV_G + e(\eta - 0.5)V_B$. From this expression for $\tilde{\epsilon}_0$ it follows that in the case of asymmetric bias-voltage drop across the junction, $\eta = 0$, the energy of the unoccupied electron level will be centered around the electrochemical potential of the right lead and moved away from this value through the gate voltage. This ingredient will be crucial for the effect addressed in this paper because the additional presence of the polaron shift will then fix the energy of the occupied (charged) state below the electrochemical potential of the right lead resulting in a blocked charged state under appropriate parameter conditions. In the case of symmetric voltage drop, $\eta = 0.5$, the energy of the unoccupied electron level will be centered around the zero of the energy resulting in a different scenario for what concerns the memory effect. In this paper, we consider the case of an asymmetric junction for which we show that the memory effect occurs for small bias voltage in a wide range of the parameters entering the model Hamiltonian (1). The symmetric situation can also give rise to a hysteretic behavior but only at finite bias voltages, making this case less interesting for the memory effect addressed here.

2.2. Spectral function, average charge and current

To obtain physical information from the Hamiltonian (1) we use the Green function method within the EOM formalism. This method is an alternative to the Green function techniques earlier applied to the considered problem in [20], [23]–[25]. We start with the retarded Green function for two generic operators a and b which is defined as

$$G^r(t_1, t_2) = -i\Theta(t_1 - t_2)\langle\{a(t_1), b(t_2)\}\rangle, \quad (3)$$

where $\langle,\rangle$ denotes a thermal average and $\{a, b\} = ab + ba$ is the anti-commutator. For the stationary case, the general expression (3) reduces to an object with only one time argument,

$$G^r(t) = -i\Theta(t)\langle\{a(t), b\}\rangle. \quad (4)$$

For a single-level system the retarded Green function in equation (4) is obtained by replacing the generic operators a and b by the electronic operators. For the Hamiltonian (1), this reads

$$G^r(t) = -\mathrm{i}\Theta(t)\left\langle\left\{d(t), d^\dagger\right\}\right\rangle. \tag{5}$$

From equation (5) one obtains the spectral function $A(\epsilon)$ of the system through the expression

$$A(\epsilon) = -2\mathrm{Im}G^r(\epsilon), \tag{6}$$

where $G^r(\epsilon)$ is the Fourier transform of $G^r(t)$. The spectral function is the basic ingredient for obtaining the transport properties of the system such as average current and charge on the molecule. The expression for the current through the molecule is given by

$$I = \frac{e\Gamma_\mathrm{L}\Gamma_\mathrm{R}}{\Gamma_\mathrm{L}+\Gamma_\mathrm{R}}\int_{-\infty}^{+\infty} A(\epsilon)\left[f_\mathrm{L}^0(\epsilon - e\varphi_\mathrm{L}) - f_\mathrm{R}^0(\epsilon - e\varphi_\mathrm{R})\right]\frac{\mathrm{d}\epsilon}{2\pi}, \tag{7}$$

where f_i^0 is the equilibrium Fermi function in the ith lead. The tunneling couplings to the right (Γ_R) and left (Γ_L) leads are

$$\Gamma_i(\epsilon) = 2\pi\sum_k |V_{i,k}|^2\delta(\epsilon - \epsilon_{i,k}), \tag{8}$$

where the matrix elements $V_{i,k}$ are assumed to be energy independent (wide-band limit). The full level broadening is given by the sum $\Gamma = \Gamma_\mathrm{L} + \Gamma_\mathrm{R}$. Below Γ_R and Γ_L are assumed to be the same.

The average charge (number of electrons), $n = \langle d^\dagger d\rangle$, is given by

$$n = \int_{-\infty}^{+\infty} A(\epsilon) f(\epsilon)\frac{\mathrm{d}\epsilon}{2\pi}, \tag{9}$$

where $f(\epsilon)$ is the distribution function of electrons inside the molecule. For the approximations used in this paper, we employ the same distribution function as in the non-interacting case,

$$f(\epsilon) = \frac{\Gamma_\mathrm{L} f_\mathrm{L}^0(\epsilon - e\varphi_\mathrm{L}) + \Gamma_\mathrm{R} f_\mathrm{R}^0(\epsilon - e\varphi_\mathrm{R})}{\Gamma_\mathrm{L}+\Gamma_\mathrm{R}}, \tag{10}$$

because we are focusing on the case of intermediate molecule–lead coupling. Fast tunneling into and out of the molecule makes plausible the assumption that the electrons are in a strong nonequilibrium situation and can then be described via equation (10) that is obtained assuming only elastic processes. Moreover, within the first approximation that we discuss in the paper, it is possible to obtain the distribution function (10) analytically by calculating the lesser Green function of the problem or applying the Hartree approximation directly to the Hamiltonian as in [20].

For a more complete explanation of the basic formulae introduced here the reader is referred to [28]–[30].

3. EOM method

3.1. General formalism

The EOMs for nonequilibrium Green functions are obtained from the Heisenberg equation for a Heisenberg operator $a(t)$,

$$\mathrm{i}\frac{\partial a}{\partial t} = [a, \hat{H}]_- = a\hat{H} - \hat{H}a. \tag{11}$$

Here and below all Hamiltonians are assumed to be time independent because we consider the stationary problem, the applied voltages enter the problem only as time-independent parameters, changing the position of the molecular energy level and the electrochemical potentials in the left and the right leads. With equation (11) the time derivative of the Green function, equation (4), reads

$$\mathrm{i}\frac{\partial G^r(t)}{\partial t} = \delta(t)\,\langle\{a(t), b\}\rangle - \mathrm{i}\Theta(t)\,\langle\{[a, H](t), b\}\rangle. \tag{12}$$

After performing a Fourier transform of equation (12), we obtain

$$(\epsilon + \mathrm{i}\eta)\,\langle\langle a, b\rangle\rangle = \langle\{a, b\}\rangle + \langle\langle [a, H], b\rangle\rangle, \tag{13}$$

where $\langle\langle,\rangle\rangle$ indicates the Fourier transform of a given Green function. Equation (13) is the starting point for the EOM method. By applying successively a time derivative there are new high-order Green functions appearing. The idea of the EOM method is thereby to truncate this iterative process at some point making the mean-field like approximation of the highest order Green function through lower order functions, in order to obtain a closed set of equations. In our case, we start from the Hamiltonian (1) and consider the first-order equation for the function $\langle\langle d, d^\dagger\rangle\rangle$ and second-order equations for the functions $\langle\langle xd, d^\dagger\rangle\rangle$ and $\langle\langle pd, d^\dagger\rangle\rangle$.

3.2. EOM method for the single-level electron–vibron Hamiltonian

The EOM method for Hamiltonian (1) generates the expressions

$$(\epsilon + \mathrm{i}\eta)\left\langle\left\langle d, d^\dagger\right\rangle\right\rangle = 1 + \tilde{\epsilon}_0\left\langle\left\langle d, d^\dagger\right\rangle\right\rangle + \lambda\left\langle\left\langle xd, d^\dagger\right\rangle\right\rangle + \sum_{i,k} V^*_{i,k}\left\langle\left\langle c_{i,k}, d^\dagger\right\rangle\right\rangle, \tag{14}$$

$$(\epsilon + \mathrm{i}\eta - \epsilon_{i,k})\left\langle\left\langle c_{i,k}, d^\dagger\right\rangle\right\rangle = V_{i,k}\left\langle\left\langle d, d^\dagger\right\rangle\right\rangle. \tag{15}$$

The equation for $\langle\langle c_{i,k}, d^\dagger\rangle\rangle$ is closed (including only the function $\langle\langle d, d^\dagger\rangle\rangle$). By substituting equation (15) into (14) and introducing the self-energy Σ of the leads through

$$\Sigma = \sum_{i,k}\frac{|V_{i,k}|^2}{\epsilon + \mathrm{i}\eta - \epsilon_{i,k}}, \tag{16}$$

we obtain eventually

$$(\epsilon + \mathrm{i}\eta - \tilde{\epsilon}_0 - \Sigma)\left\langle\left\langle d, d^\dagger\right\rangle\right\rangle = 1 + \lambda\left\langle\left\langle xd, d^\dagger\right\rangle\right\rangle. \tag{17}$$

The last term, describing the interaction between electron and vibron, has to be truncated at this level or found from higher order equations and then truncated at a higher level of approximation. The lead self-energy will be used below in the wide-band approximation $\Sigma(\epsilon) = -\mathrm{i}\Gamma$.

3.3. Self-consistent Hartree approximation

The simplest way to close equation (17) is to perform the truncation by approximating

$$\left\langle\left\langle xd, d^\dagger\right\rangle\right\rangle \approx \langle x\rangle\left\langle\left\langle d, d^\dagger\right\rangle\right\rangle. \tag{18}$$

Then we obtain immediately for the Green function

$$G^r_{\mathrm{H}}(\epsilon) = \left\langle\left\langle d, d^\dagger\right\rangle\right\rangle = \frac{1}{\epsilon - \tilde{\epsilon}_0 - \lambda\langle x\rangle + \mathrm{i}\Gamma}. \tag{19}$$

Here the quantity $\langle x\rangle$ remains to be calculated. To this end we compute, respectively, the time derivatives of the x-operator,

$$\mathrm{i}\frac{\partial x}{\partial t} = [x, H] = \omega_0 p \tag{20}$$

and the p-operator,

$$\mathrm{i}\frac{\partial p}{\partial t} = \omega_0 x + 2\lambda d^\dagger d. \tag{21}$$

Upon combining equations (20) and (21), we get

$$-\frac{\partial^2 x}{\partial t^2} = \omega_0^2 x + 2\lambda\omega_0 d^\dagger d. \tag{22}$$

In the stationary case addressed, equation (22) yields a direct connection between the 'position' of the vibron and the particle number in the dot:

$$\langle x\rangle = -2\frac{\lambda}{\omega_0}\left\langle d^\dagger d\right\rangle = -2\frac{\lambda}{\omega_0} n. \tag{23}$$

In view of equation (19), we finally obtain for the spectral function (6) the following self-consistent expression:

$$A(\epsilon) = \frac{2\Gamma}{\left(\epsilon - \tilde{\epsilon}_0 + 2(\lambda^2/\omega_0)n\right)^2 + \Gamma^2}\,. \tag{24}$$

This result is equivalent to the one obtained earlier in [20, 24, 25] using alternative approaches. The same spectral function can be found if one takes the self-energy in Hartree approximation.

3.4. Second approximation

In the first approximation above, the self-consistent Hartree treatment, fluctuations of the particle number n and the vibron coordinate x are completely neglected. In order to go one step further and estimate possible corrections, we start from the generated equations for the second-order Green functions, $\langle\langle xd, d^\dagger\rangle\rangle$ and $\langle\langle pd, d^\dagger\rangle\rangle$,

$$(\epsilon + \mathrm{i}\eta - \tilde{\epsilon}_0)\left\langle\left\langle xd, d^\dagger\right\rangle\right\rangle = \langle x\rangle + \omega_0\left\langle\left\langle pd, d^\dagger\right\rangle\right\rangle + \lambda\left\langle\left\langle x^2 d, d^\dagger\right\rangle\right\rangle + \sum_{i,k} V^*_{i,k}\left\langle\left\langle xc_{i,k}, d^\dagger\right\rangle\right\rangle, \tag{25}$$

$$(\epsilon + \mathrm{i}\eta - \tilde{\epsilon}_0)\left\langle\left\langle pd, d^\dagger\right\rangle\right\rangle = \omega_0\left\langle\left\langle xd, d^\dagger\right\rangle\right\rangle + \lambda\left\langle\left\langle pxd, d^\dagger\right\rangle\right\rangle + \sum_{i,k} V^*_{i,k}\left\langle\left\langle pc_{i,k}, d^\dagger\right\rangle\right\rangle. \tag{26}$$

The second approximation that we consider here is based on the factorization

$$\begin{aligned}
&\left\langle\left\langle x^2 d, d^\dagger\right\rangle\right\rangle \approx \langle x\rangle\left\langle\left\langle xd, d^\dagger\right\rangle\right\rangle,\\
&\left\langle\left\langle pxd, d^\dagger\right\rangle\right\rangle \approx \langle x\rangle\left\langle\left\langle pd, d^\dagger\right\rangle\right\rangle + 2\left\langle\left\langle d, d^\dagger\right\rangle\right\rangle,\\
&\left\langle\left\langle xc_{i,k}, d^\dagger\right\rangle\right\rangle \approx \langle x\rangle\left\langle\left\langle c_{i,k}, d^\dagger\right\rangle\right\rangle,\\
&\left\langle\left\langle pc_{i,k}, d^\dagger\right\rangle\right\rangle \approx 0.
\end{aligned} \tag{27}$$

The corresponding set of equations reads

$$\begin{aligned}
(\epsilon + \mathrm{i}\eta - \tilde{\epsilon}_0 - \Sigma)\left\langle\left\langle d, d^\dagger\right\rangle\right\rangle &= 1 + \lambda\left\langle\left\langle xd, d^\dagger\right\rangle\right\rangle,\\
(\epsilon + \mathrm{i}\eta - \tilde{\epsilon}_0 - \lambda\langle x\rangle)\left\langle\left\langle xd, d^\dagger\right\rangle\right\rangle &= \langle x\rangle + \omega_0\left\langle\left\langle pd, d^\dagger\right\rangle\right\rangle + \langle x\rangle\,\Sigma\left\langle\left\langle d, d^\dagger\right\rangle\right\rangle,\\
(\epsilon + \mathrm{i}\eta - \tilde{\epsilon}_0 - \lambda\langle x\rangle)\left\langle\left\langle pd, d^\dagger\right\rangle\right\rangle &= \omega_0\left\langle\left\langle xd, d^\dagger\right\rangle\right\rangle + 2\lambda\left\langle\left\langle d, d^\dagger\right\rangle\right\rangle,
\end{aligned} \tag{28}$$

from which we obtain the second approximation for the Green function,

$$\left[G^r(\epsilon)\right]^{-1} = \left[G^r_{\mathrm{H}}(\epsilon)\right]^{-1} - \left(\lambda\,\langle x\rangle + \frac{\lambda^2}{\omega_0}\right)\frac{\Omega}{\Delta-\Omega}, \tag{29}$$

where we introduced $\Delta = \epsilon + \mathrm{i}\eta - \tilde{\epsilon}_0$, $\Omega = \frac{\omega_0^2}{\Delta - \lambda\langle x\rangle}$, and G^r_{H} is given by the Green function obtained in the Hartree approximation, equation (19). After inserting the expression (23) for the level population $\langle x\rangle$, equation (29) reads

$$\left[G^r(\epsilon)\right]^{-1} = \left[G^r_{\mathrm{H}}(\epsilon)\right]^{-1} - (1-2n)\,\frac{\lambda^2}{\omega_0}\,\frac{\Omega}{\Delta-\Omega}. \tag{30}$$

We then calculate the spectral function (6) and the average number of electrons (9). The self-consistent calculation is performed following the chain $G^r(\epsilon) \to A(\epsilon) \to n \to G^r(\epsilon)$.

Before entering into the discussion of the calculated quantities, we consider the structure of the Green functions obtained in the two different approximations:

- In the limit where $\Omega \to 0$ the second approximation reduces to the first one. Although the EOM method is not a systematic expansion, it tells us that the second approximation consistently extends the first one and reproduces it in a limiting case.
- The second term on the right-hand side of equation (30) represents an additional shift with respect to equation (19). In the case of very small frequencies ω_0, equation (30) reduces to $[G^r_{\mathrm{H}}(\epsilon)]^{-1} - (1-2n)\lambda^2\frac{\omega_0}{\Delta(\Delta-\lambda\langle x\rangle)}$, involving the first term of a series expansion in ω_0.

4. Results, discussion and conclusions

Starting from the expressions derived above within the first (self-consistent Hartree) and second approximation, we have performed numerical simulations for the average population and current in the molecular junction as a function of gate and bias voltage for the different parameters λ, Γ and T entering the model Hamiltonian. Furthermore, we compare the two approximations. The underlying nonlinear equations give rise to bistability in the level population thereby enabling memory effects and affecting the current. Below we analyze in detail the parameter ranges and conditions for memory effects to occur. We focus here on the case of an asymmetric junction, $\eta = 0$, while keeping the coupling to the leads symmetric, $\Gamma_{\mathrm{L}} = \Gamma_{\mathrm{R}} = \Gamma$, to reduce the parameter space.

First, we investigate the gate-voltage dependence of the level population. In figure 2, it is clearly seen that bistability takes place only at larger values of the electron–vibron coupling λ. The critical values at which bistability occurs and disappears depend on the coupling Γ to the leads and on temperature T; we discuss this parameter dependence below. Note that at large values of λ the level population of the stable states is close to 0 and 1; thus these two memory states are well distinguishable in charge.

A comparison between the left and right panels of figure 2, representing the two different levels of approximations in the EOM method, shows that the self-consistent Hartree treatment underestimates the parameter range where bistability occurs: the critical value of λ for the occurrence of bistable behavior is close to $3\omega_0$ (see left panel). At this value a bistable regime has already developed for the second approximation. This can be partially understood taking into account the additional term appearing in the Green function for the second approximation, equation (30). This term increases the polaron shift thereby enhancing the bistable behavior in

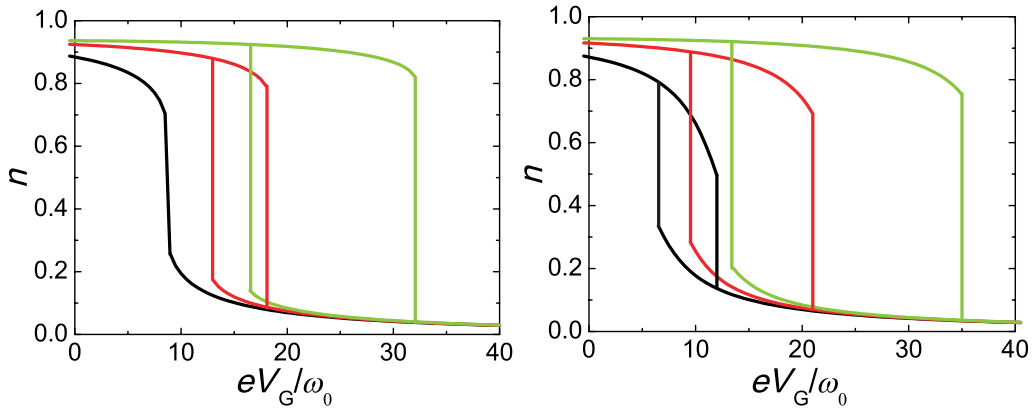

Figure 2. Bistable behavior of the level population n in the self-consistent Hartree approximation (left) and second approximation (right) as a function of *gate* voltage for different electron–vibron interaction strength $\lambda = 3\omega_0$ (black), $\lambda = 4\omega_0$ (red), $\lambda = 5\omega_0$ (green), the other parameters are $\Gamma = 5\omega_0$, $T = 0.25\omega_0$, $\eta = 0$ and $V_B = 0$.

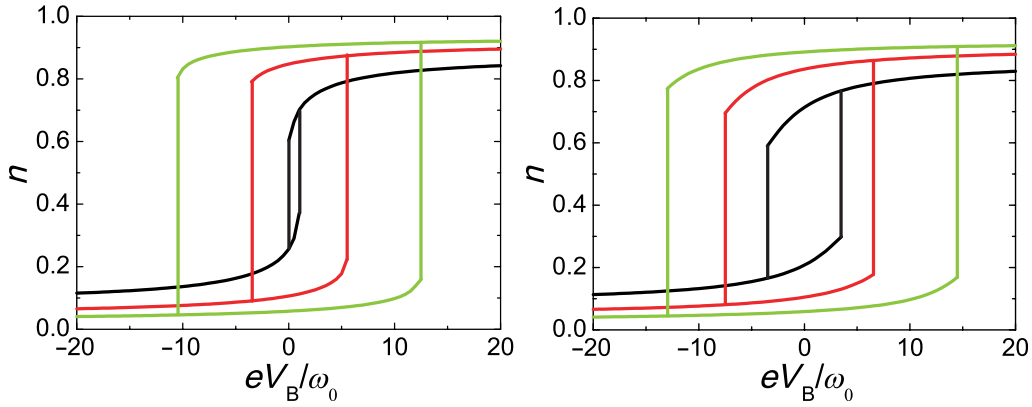

Figure 3. Level population n in the self-consistent Hartree approximation (left) and the second approximation (right) as a function of normalized *bias* voltage for different electron–vibron interaction strength $\lambda = 3\omega_0$ (black), $\lambda = 4\omega_0$ (red), $\lambda = 5\omega_0$ (green), the other parameters are $\Gamma = 5\omega_0$, $T = 0.25\omega_0$, $\eta = 0$ and $V_G = \frac{\lambda^2}{\omega_0}$.

the second approximation. Figure 3 shows the bias-voltage dependence of the level population. In this case, a qualitative difference arises between electrostatically symmetric ($\eta = 0.5$) and asymmetric ($\eta = 0$) junctions. For asymmetric junctions both states are stable at zero voltage, and both charge states are easily accessible. As we showed recently [23], asymmetric junctions are thus favorable, since they exhibit memory effects and hysteretic behavior at zero bias, enabling controlled switching upon ramping the bias voltage. For symmetric junctions, hysteresis is expected only at finite bias voltage (nonequilibrium bistability [20]), and hence only a single stable state exists at zero bias. Furthermore, at finite voltage the level is only partially occupied by tunneling electrons. These two features render the symmetric system less suited for a memory setup.

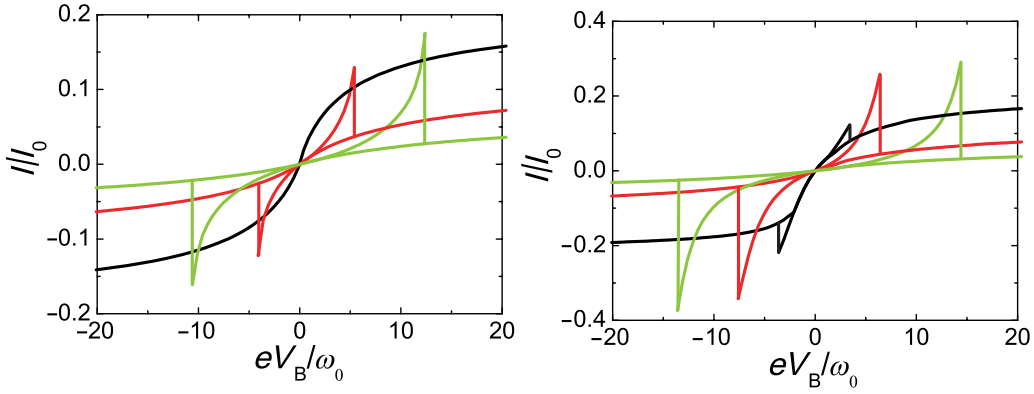

Figure 4. Current normalized to $I_0 = \Gamma e/4$ versus bias voltage for the self-consistent Hartree approximation (left) and the second approximation (right) for different electron–vibron interaction strength $\lambda = 3\omega_0$ (black), $\lambda = 4\omega_0$ (red), $\lambda = 5\omega_0$ (green), for the same parameters as in figure 3.

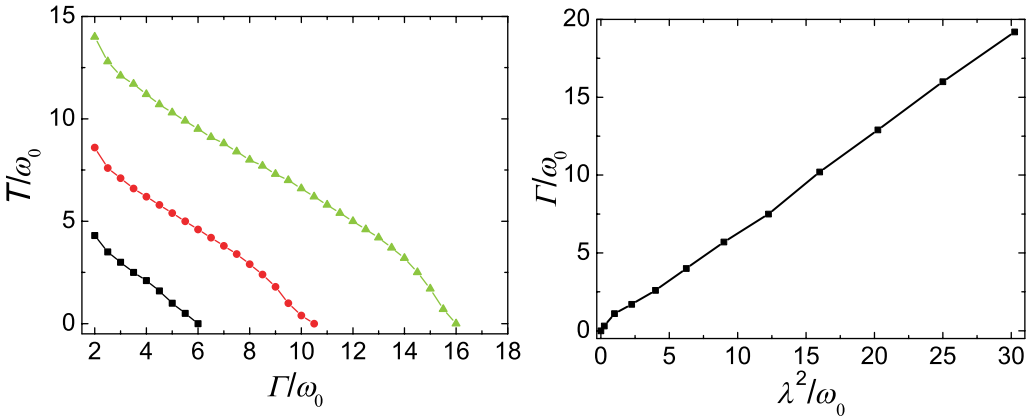

Figure 5. 'Phase diagram' depicting the boundaries between parameter regimes of bistable memory (below the threshold lines) and single-valued states (above threshold). Left panel: $\Gamma - T$ parameter plane at different electron–vibron interaction strength $\lambda = 3\omega_0$ (black), $\lambda = 4\omega_0$ (red), $\lambda = 5\omega_0$ (green); right panel: $\lambda - \Gamma$ parameter plane for $T = 0.25\omega_0$.

We further display in figure 4 the current–voltage characteristics, which reflects the switching behavior of the system. The characteristic feature is a current jump at the bias voltage value where recharging sets in. This behavior can be used to test the state of the system and as readout.

Finally, we depict in figure 5 'phase diagrams' showing the boundaries between the parameter regions where bistable memory states (below the boundaries in the two panels of figure 5) and single-valued states exist. The left panel of figure 5 shows the $\Gamma - T$ parameter plane. The curve separating single-valued and bistable states can be roughly approximated by the condition $\Gamma + T = c(\lambda)$, where $c(\lambda)$ is extracted to be $c(\lambda) \approx \lambda^{1.7}$. This means that either thermal or quantum tunneling broadening suppresses the hysteresis. The disappearance of the memory effect at high temperature is due to enhanced electron tunneling into the higher

energy state. We note that in the analysis of the temperature dependence the effect of vibronic coordinate fluctuations is neglected that can be relevant close to the threshold between single-valued and bistable regime. The right panel in figure 5, displaying the $\lambda^2 - \Gamma$ parameter plane, shows on the one hand that bistable behavior requires, for growing Γ, increasing electron–vibron coupling λ. The boundary between the two regimes is approximately a straight line in the $\lambda^2 - \Gamma$ plane. Hence, the condition for finding the memory effect is given by $\Gamma \leqslant 0.63\lambda^2/\omega_0$. This clearly shows that for the appearance of the memory effect at low temperature, the two energy scales to be compared are the level broadening Γ and the polaron shift λ^2/ω_0. A further important conclusion is that the memory effect is suppressed for large coupling to the leads. Since, on the other hand, larger coupling favors fast information writing and reading and also can additionally suppress effects from quantum tunneling between states, the problem arises to find optimal parameters for utilizing the memory effect. This will be the subject of future work.

To conclude, we considered a *charge-memory effect* and switching phenomena within a single-level polaron model of a molecular junction in the framework of the EOM approach to the nonequilibrium Green function theory at different levels of approximation. Electrostatically symmetric and asymmetric junctions show qualitatively different bistability behavior. In the latter case, controlled switching of the molecule is achieved by applying finite voltage pulses. We showed that bistability takes place for sufficiently large electron–vibron coupling for a wide range of further parameters such as molecule–lead coupling and temperature and performed a systematic analysis of this parameter dependence by computing phase diagrams for the memory effect. We focused on the investigation of bistability for stationary states, leaving the problem of time-dependent fluctuations and fluctuation-induced switching as an open question to be investigated in future research.

Acknowledgments

We acknowledge fruitful discussions with J Repp and thank one of the referees for useful hints. This work was funded by the Deutsche Forschungsgemeinschaft within Priority Program SPP 1243, Collaborative Research Center SFB 689 (DAR) and within the international collaboration ‘Single molecule based memories’ CU 44/3-2 (DAR).

References

[1] Reed M A and Tour J M 2000 Computing with molecules *Sci. Am.* **282** 86
[2] Nitzan A and Ratner M A 2003 Electron transport in molecular wire junctions *Science* **300** 1384
[3] Joachim C and Ratner M A 2005 Molecular electronics: some views on transport junctions and beyond *Proc. Natl Acad. Sci. USA* **102** 8801
[4] Cuniberti G, Fagas G and Richter K (ed) 2005 *Introducing Molecular Electronics* (Berlin: Springer)
[5] Park H, Park J, Lim A K L, Anderson E H, Alivisatos A P and McEuen P L 2000 Nanomechanical oscillations in a single-C_{60} transistor *Nature* **407** 57
[6] Smit R H M, Noat Y, Untiedt C, Lang N D, van Hemert M C and van Ruitenbeek J M 2002 Measurement of the conductance of a hydrogen molecule *Nature* **419** 906
[7] Yu L H, Keane Z K, Ciszek J W, Cheng L, Stewart M P, Tour J M and Natelson D 2004 Inelastic electron tunneling via molecular vibrations in single-molecule transistors *Phys. Rev. Lett.* **93** 266802
[8] Qiu X H, Nazin G V and Ho W 2004 Vibronic states in single molecule electron transport *Phys. Rev. Lett.* **92** 206102

[9] Osorio E A, O'Neill K, Stuhr-Hansen N, Nielsen O F, Bjrnholm T and van der Zant H S J 2007 Addition energies and vibrational fine structure measured in electromigrated single-molecule junctions based on an oligophenylenevinylene derivative *Adv. Mater.* **19** 281
[10] Lörtscher E, Weber H B and Riel H 2007 Statistical approach to investigating transport through single molecules *Phys. Rev. Lett.* **98** 176807
[11] Lörtscher E, Ciszek J W, Tour J and Riel H 2006 Reversible and controllable switching of a single-molecule junction *Small* **2** 973
[12] del Valle M, Gutiérrez R, Tejedor C and Cuniberti G 2007 Tuning the conductance of a molecular switch *Nat. Nanotechnol.* **2** 176
[13] Choi B-Y, Kahng S-J, Kim S, Kim H, Kim H W, Song Y J, Ihm J and Kuk Y 2006 Conformational molecular switch of the azobenzene molecule: a scanning tunneling microscopy study *Phys. Rev. Lett.* **96** 156106
[14] Martin M, Lastapis M, Riedel D, Dujardin G, Mamatkulov M, Stauffer L and Sonnet P 2006 Mastering the molecular dynamics of a bistable molecule by single atom manipulation *Phys. Rev. Lett.* **97** 216103
[15] Liljeroth P, Repp J and Meyer G 2007 Current-induced hydrogen tautomerization and conductance switching of naphthalocyanine molecules *Science* **317** 1203–6
[16] Koch J and von Oppen F 2005 Franck–Condon blockade and giant fano factors in transport through single molecules *Phys. Rev. Lett.* **96** 206804
[17] Repp J, Meyer G, Olsson F E and Persson M 2004 Controlling the charge state of individual gold adatoms *Science* **305** 493
[18] Olsson F E, Paavilainen S, Persson M, Repp J and Meyer G 2007 Multiple charge states of Ag atoms on ultrathin NaCl films *Phys. Rev. Lett.* **98** 176803
[19] Alexandrov A S and Bratkovsky A M 2003 Memory effect in a molecular quantum dot with strong electron–vibron interaction *Phys. Rev.* B **67** 235312
[20] Galperin M, Ratner M A and Nitzan A 2005 Hysteresis, switching, and negative differential resistance in molecular junctions: a polaron model *Nano Lett.* **5** 125
[21] Mitra A, Aleiner I and Millis A J 2005 Semiclassical analysis of the nonequilibrium local polaron *Phys. Rev. Lett.* **94** 076404
[22] Mozyrsky D, Hastings M B and Martin I 2006 Intermittent polaron dynamics: Born–Oppenheimer approximation out of equilibrium *Phys. Rev.* B **73** 035104
[23] Ryndyk D A, D'Amico P, Cuniberti G and Richter K 2008 Charge-memory effect in molecular junctions *Phys. Rev.* B at press (*Preprint* 0802.2808v1)
[24] Hewson A C and Newns D M 1974 Effect of the image force in chemisorption *Japan. J. Appl. Phys. Suppl.* **2** 121
[25] Hewson A C and Newns D M 1979 Polaronic effectnin mixed- and intermediate-valence compounds *J. Phys. C: Solid State Phys.* **12** 1665
[26] Meir Y and Wingreen N S 1992 Landauer formula for the current through an interacting electron region *Phys. Rev. Lett.* **68** 2512
[27] Jauho A-P, Wingreen N S and Meir Y 1994 Time-dependent transport in interacting and noninteracting resonant-tunneling systems *Phys. Rev.* B **50** 5528
[28] Haug H and Jauho A-P 1996 *Quantum Kinetics and Optics of Semiconductors (Springer Series in Solid-State Sciences* vol 123) (Berlin: Springer)
[29] Bruus H and Flensberg K 2004 *Many-Body Quantum Theory in Condensed Matter Physics* (Oxford: Oxford University Press)
[30] Ryndyk D A, Gutiérrez R, Song B and Cuniberti G 2008 Green function techniques in the treatment of quantum transport at the molecular scale submitted to *Springer Series* '*Lecture Notes in Physics*' (*Preprint* 0805.0628)